第51卷第11期 中国科学技术大学学报 Vol. 51, No. 11
2021年11月 JOURNAL OF UNIVERSITY OF SCIENCE AND TECHNOLOGY OF CHINA Nov. 2021
Received: 2021-03-05; Revised: 2021-04-08 doi:10.52396/JUST-2021-0088

A novel amidoxime modified polyethylene nanofibrous membrane with high uranium adsorption capacity

YU Rui[1], WAN Caixia[1], CHEN Xin[1,2*], LI Liangbin[1*]

1. National Synchrotron Radiation Laboratory, Anhui Provincial Engineering Laboratory of Advanced Functional Polymer Film, CAS Key Laboratory of Soft Matter Chemistry, University of Science and Technology of China, Hefei 230026, China;
2. National Co-Innovation Center for Nuclear Waste Disposal and Environmental Safety, Southwest University of Science and Technology, Mianyang 621010, China
* Corresponding author. E-mail: cx1003@ustc.edu.cn; lbli@ustc.edu.cn

Abstract: The amidoxime modified polyethylene nanofibrous membrane (AO-PENFM) was prepared by a two-step graft polymerization method and an amidoximation reaction. Firstly, the hydroxyethyl acrylate (HEA) was grafted on polyethylene nanofibrous membrane (PENFM) via pre-radiation induced graft polymerization, then the acrylonitrile (AN) and acrylic acid (AA) were grafted on poly hydroxyethyl acrylate (PHEA) chains by ceric ammonium nitrate (CAN) initiated graft polymerization. Finally, an aminoximation reaction was performed to prepare the novel AO-PENFM adsorbent. This two-step graft method was used to construct a nanostructure adsorption layer with high specific surface areas on the surface of PENFM. The AO-PENFM adsorbent in a uranium solution of 12 ppm after 120 h adsorption performs an excellent adsorption performance of 338.14 mg/g. Simultaneously, the adsorption kinetics conforms to the intraparticle diffusion model and pseudo-second-order model. In addition, the adsorption isotherm data conform to the Langmuir isotherm model.

Keywords: polyethylene nanofibrous membrane; pre-radiation induced graft polymerization; CAN initiated graft polymerization; uranium adsorption

CLC number: TL212; TQ424; TQ342+.61 **Document code**: A

1 Introduction

Uranium, the basic element for nuclear power plants, exists in nature in two main forms: dissolved in ocean and deposited in minerals on land[1-3]. Uranium mainly exists in the form of uranyl carbonate in seawater, with a much lower concentration of 3.3 ppb. About 4.5 billion tons of uranium are estimated to be in the ocean, about 1,000 times as much as on land[4,5]. Thus, uranium extraction from seawater offers a very promising alternative to meet nuclear fuel needs. However, the biggest challenge of uranium extraction from seawater is the adsorption capacity of adsorbents is relatively low, due to the much lower uranium concentration in seawater. To overcome this challenge, adsorbents with higher adsorption capacity are required.

There are many methods to extract uranium from seawater, such as ionic exchange[6,7], electrochemical[8], coprecipitation[9] and adsorption[5,8,10-28]. Because of its advantages of low costs, easy operation, simple recovery and high adsorption efficiency, the adsorption method, especially using the polymer-based adsorbents, is highly recommended. For economic and viable extraction of uranium from seawater, adsorbents must have an efficient adsorption capacity. There are two ways to improve the uranium adsorption capacity. One is to search for functional ligands that can adsorb uranium effectively. The amidoxime group is the functional group that was selected to extract uranium from seawater[4,13,29-31]. It has an outstanding chelating affinity and selectivity for uranyl ions. The other is to look for new materials with large specific surface areas[12,15,24,32,33]. Meanwhile, it would be better to increase the specific surface area of the adsorption sites rather than that of the matrix material[32].

Various materials have been used to study uranium extraction from seawater, including mesoporous silica[25], metal organic framework[25], cellulose[35], hydrogel[14,36] and fiber[4,37-39]. Due to its advantages of low costs and easy operation, polymer-based matrix materials are widely chosen to extract uranium from

Citation: Yu Rui, Wan Caixia, Chen Xin, et al. A novel amidoxime modified polyethylene nanofibrous membrane with high uranium adsorption capacity. J. Univ. Sci. Tech. China, 2021, 51(11): 831-839.

seawater. At present, there are many polymer-based matrix materials for uranium extraction, such as polyolefin fiber materials[4, 18, 23, 37-39], polyacrylonitrile fiber[20, 40, 41] and so on. Increasing the specific surface area of fiber materials, such as hollow fibers and gear fibers, will inevitably lead to the decline of mechanical properties of fiber materials. Polyolefin membrane materials can avoid the problem of mechanical property degradation. However, polyolefin nanofibrous membrane is rarely used as the matrix material for uranium adsorption. Because of the large specific surface area and excellent mechanical properties, polyolefin nanofibrous membrane is a good matrix material for uranium adsorption.

In this work, a novel amidoxime (AO)-modified PENFM (AO-PENFM) adsorbent was prepared via pre-radiation induced graft polymerization (RIGP) and CAN initiated graft polymerization (CIGP) (Scheme 1). The AO-PENFM has a unique nanostructure adsorption layer with high specific surface areas. Therefore, a mass of adsorption sites were constructed on the AO-PENFM adsorbent surface. PENFM-g-PHEA obtained via RIGP and AO-PENFM via CIRP was characterized by XPS, FT-IR and SEM. These results showed that HEA, AN and AA were modified to the PENFM surface. Adsorption tests were performed in 12 ppm uranium spiked solution to test the adsorption capacity of AO-PENFM andobtain excellent adsorption capacity of 338. 14 mg/g after 120 h adsorption.

2 Experimental

2.1 Materials

The PENFM is homemade, and the detailed process refers to previous paper[42, 43]. Copper (II) sulfate pentahydrate ($CuSO_4 \cdot 5H_2O$), hydroxyethyl acrylate (HEA), nitric acid (HNO_3), ceric ammonium nitrate (CAN), acrylic acid (AA), acrylonitrile (AN), hydroxylamine hydrochloride ($NH_2OH \cdot HCl$), N, N-dimethylformamide (DMF), methanol (CH_3OH) and potassium hydroxide (KOH) bought from Sinopharm Chemical Reagent Company were reagent grade and used as received. The uranium solution used for adsorption experiments was prepared by dissolving proper amount of $UO_2(NO_3)_2 \cdot 6H_2O$ into deionized water.

2.2 Synthesis of AO-PENFM adsorbents

The novel amidoxime-modified nanofibrous membrane adsorbent, denoted as AO-PENFM, was synthesized as follows: ① Firstly, the PENFM samples were irradiated with ^{60}Co γ-ray (7.4×10^{15} Bq, located in the University of Science and Technology of China) at a dose rate 76.4 Gy/min in air at room temperature. ②Secondly, RIGP of HEA is processed in flasks containing 25%/75% (volume fraction) HEA/H_2O and 1 mmol/L $CuSO_4 \cdot 5H_2O$ at 70 ℃ (called as PENFM-g-PHEA). ③Subsequently, CIGP of AN/AA is processed in a flask containing 40%/48%/12% (volume fraction) DMF/AN/AA and 5 mL stock CAN solution (0.1 mol/L CAN in 1 mol/L HNO_3) at 50 ℃ (called as PENFM-g-PHEA-(PAN-co-PAA)). ④ Then, a 10% (mass fraction) $NH_2OH \cdot HCl$ solution used for amidoximation reaction was prepared using 50%/50% (volume fraction) H_2O/CH_3OH, and KOH was added to adjust the pH to neutral. After that, PENFM-g-PHEA-(PAN-co-PAA) was added to the above solution and stirred at 70 ℃ for 4 h. After amidoximation reaction, the samples were called as AO-PENFM. Before using for uranium extraction, the AO-PENFM adsorbents were incubated in 2.5% (mass fraction) KOH solution at 80 ℃ for 3 h, then rinsed with deionized water before using for uranium adsorption.

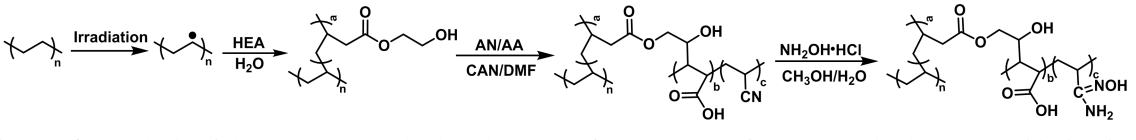

Scheme 1. Synthesis of the AO-PENFM adsorbent by RIGP of HEA, CIGP of AN/AA and subsequent amidoximation.

2.3 Characterization methods

The XPS was analyzed by a Thermo Scientific EscaLab 250Xi instrument.

The FT-IR was analyzed using attenuated total reflection mode by a Nicolet 8700 instrument.

SEM images were taken with ZEISS GE mini SEM 500 instrument.

BET specific surface areas were analyzed using Tristar II 3020M instrument.

The Inductively coupled plasma atomic emission spectroscopy (ICP-AES) was used to analyze uranium concentration using a Perkin-Elmer Corporation Optima 7300DV instrument.

2.4 Uranium adsorption experiments

2.4.1 Kinetics experiments

The kinetics experiments were performed in 1 L glass bottles containing 12 ppm uranium spiked solution. 10.0 mg ± 1. 0 mg alkaline activated AO-PENFM was immersed in 1 L 12 ppm uranium spiked solution with shaking on a shaking bath at 25 ℃ and 100 r/min. At the specified time point, the solution was analyzed using ICP-AES. Each experiment was performed 3 times.

Equation (1) was used to calculate the uranium adsorption by AO-PENFM.

$$Q_t = (C_0 - C_t) \times \frac{V}{m} \quad (1)$$

where Q_t (mg/g) is the uranium adsorption capacity at contact time t (h); C_t (mg/L) is the uranium concentration at contact time t (h) and C_0 (mg/L) is the initial uranium concentration; m (g) is the AO-PENFM adsorbent mass and V (L) is the solution volume.

2.4.2　Isotherm experiments

A series of uranium spiked solution (1−32 ppm) were prepared firstly for the adsorption isotherm study. Then 10.0 mg±1. 0 mg alkaline activated AO-PENFM was added in 1 L a series of uranium spiked solution with shaking on a shaking bath for 24 h at 25 ℃ and 100 r/min. The solution was analyzed using ICP-AES after 24 h adsorption. Each experiment was performed 3 times.

2.4.3　Reusability of the AO-PENFM adsorbent

It is important for an economical adsorbent to be easily reusable. The adsorption-desorption test was performed in 12 ppm uranium spiked solution for six cycles. After uranium adsorption, the adsorbent adsorbed uranium was eluted with a 0. 5 mol/L HCl solution at room temperature for 1 h and regenerated with a 5 mmol/L KOH solution at the room temperature for 15 min, then washed with deionized water 3 times before the next adsorption experiment.

3　Results and discussion

3.1　Characterization of PENFM, PENFM-g-PHEA, PENFM-g-PHEA-(PAN-co-PAA) and AO-PENFM

3.1.1　FT-IR characterization

As shown in Figure 1, the FT-IR spectroscopy of the PENFM, PENFM-g-PHEA, PENFM-g-PHEA-(PAN-co-PAA) and AO-PENFM are recorded. For PENFM, the two characteristic peaks of $-CH_2-$ groups correspond to the symmetric and asymmetric stretching vibration at 2848 cm^{-1} and 2916 cm^{-1}. Meanwhile, it can be observed in all spectroscopy. For PENFM-g-PHEA, a new C=O peak appears at 1732 cm^{-1}, indicating that PHEA chains are successfully grafted onto PENFM. For PENFM-g-PHEA-(PAN-co-PAA), the new sharp peak at 2243 cm^{-1} is observed and attributed to −CN, which almost disappears after amidoximation. The appearance of the peak of −CN shows the successfully grafted AN onto PHEA chains, while the disappearance −CN peak indicates that −CN group is completely transformed into AO group after amidoximation. Meanwhile, for AO-PENFM, new characteristic peaks at 3000 to 3700, 1645 and 926 cm^{-1} are attributed to $-OH/-NH_2$, −C=N− and −N−O−, respectively.

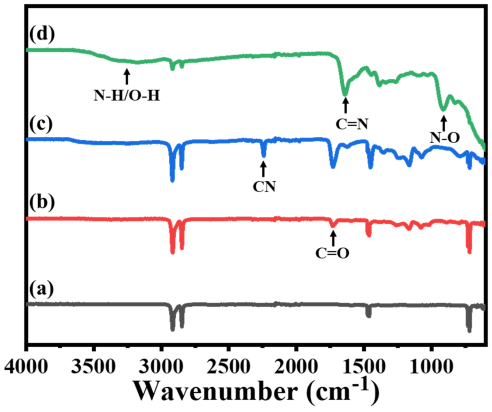

Figure 1. FT-IR spectroscopy of (a) PENFM, (b) PENFM-g-PHEA, (c) PENFM-g-PHEA-(PAN-co-PAA) and (d) AO-PENFM.

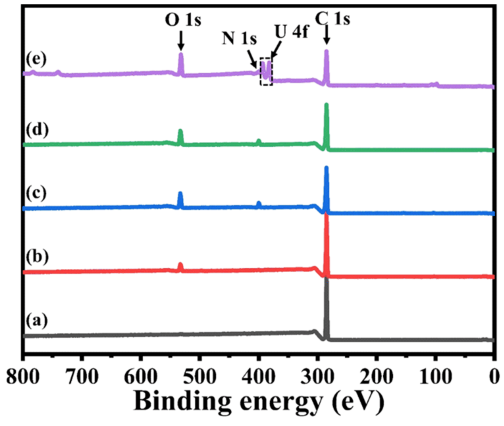

Figure 2. XPS spectroscopy of (a) PENFM, (b) PENFM-g-PHEA, (c) PENFM-g-PHEA-(PAN-co-PAA), (d) AO-PENFM and (e) AO-PENFM-U.

3.1.2　XPS characterization

The XPS spectroscopy of the PENFM, PENFM-g-PHEA, PENFM-g-PHEA-(PAN-co-PAA), AO-PENFM and AO-PENFM-U are shown in Figure 2. For PENFM, a strong peak at 285.1 eV attributed to C 1s is observed and also observed in the spectroscopy of all samples. For PENFM-g-PHEA, a new peak at 533. 1 eV attributed to O 1s is observed suggested that PHEA chains were successfully grafted onto PENFM. For PENFM-g-PHEA-(PAN-co-PAA), a new peak at 400.1 eV attributed to N 1s is observed because of the successfully grafted AN onto PHEA chains. For AO-PENFM, the peak of N 1s is shown in Figure 3(a) and the three fitting peaks at 399.5, 400.3 and 400.9 eV are attributed to N−O, C=N and N−H. And the peak of O 1s is shown in Figure 3(b) and the three fitting peaks at 531.7, 532.5 and 533.5eV are attributed to N−O, C=O and C−O. This results indicate that the surface of the membrane material has been successfully modified with AO functional groups. For AO-PENFM-U, that is short for the AO-PENFM adsorbent after uranium adsorption,

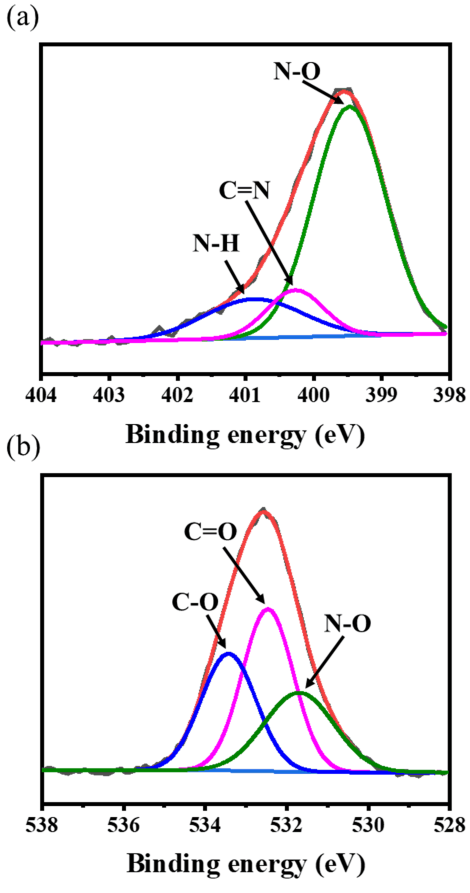

Figure 3. High-resolution XPS spectroscopy of (a) N 1s and (b) O 1s for AO-PENFM.

as shown in Figure 2(e), the characteristic peak appeared at 382.1 eV (U $4f_{7/2}$) and 392. 1 eV (U $4f_{5/2}$) are observed, which suggested the successful adsorption of uranium.

3.1.3 SEM characterization

As shown in Figure 4, the morphologies of the PENFM, PENFM-g-PHEA, PENFM-g-PHEA-(PAN-co-PAA) and AO-PENFM are characterized using SEM. For the PENFM, the surface was relatively smooth as shown in Figure 4(a). However, after grafting HEA, the morphology of the PENFM-g-PHEA is relatively rough as shown in Figure 4(b). After grafting AN/AA on PHEA molecular chains, many particle structures are generated on the membrane surface with the particle size ranging from tens to hundreds of nanometers, so nanostructures are successfully constructed on the membrane surface as shown in Figure 4(c). After amidoximation, the surface morphology of adsorbents do not change significantly as shown in Figure 4(d), indicating that the amidoximation reaction do not destroy nanostructure adsorption layer of the membrane surface. Meanwhile, nanostructures are constructed on the membrane surface to form a huge adsorption site, which is conducive to the contact between uranium and

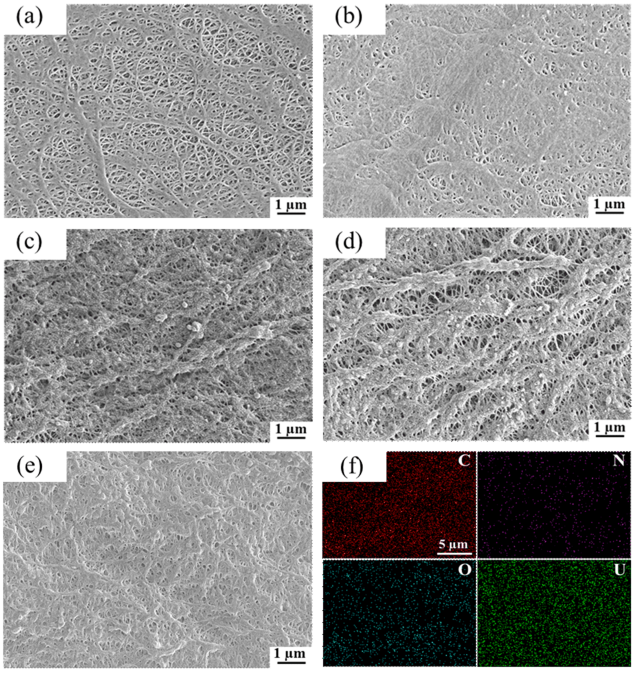

Figure 4. SEM micrographs of (a) PENFM, (b) PENFM-g-PHEA, (c) PENFM-g-PHEA-(PAN-co-PAA), (d) AO-PENFM, (e) eluted AO-PENFM and (f) EDS elemental distribution mapping images of the element of C, N, O and U of AO-PENFM after adsorption, respectively.

adsorption sites, thus having a high adsorption capacity. After uranium adsorption, the adsorbent adsorbed uranium (called as AO-PENFM-U) was eluted with a 0.5 mol/L HCl solution, and the surface morphology of the adsorbent did not change significantly as shown in Figure 4(e). In other words, the surface morphology of the adsorption layer on the membrane surface was well preserved after elution. Meanwhile, the EDS images as shown in Figure 4(f) suggest that the U is homogeneously distributed on the surface of the AO-PENFM adsorbent and further strongly prove the adsorption is relatively uniform.

3.2 Uranium adsorption study

3.2.1 Adsorption kinetics study

The uranium adsorption test of AO-PENFM was determined by soaking 10.0 mg ± 1.0 mg of alkaline activated AO-PENFM adsorbent in 1 L 12 ppm uranium spiked solution by using a constant temperature shaking bath at 25 ℃. The result shows that the AO-PENFM exhibits high adsorption capacity of 338.14 mg/g after 120 h adsorption.

To study adsorption kinetics behavior, the uranium adsorption on AO-PENFM was simulated by using the pseudo-first-order model based on physical adsorption as the rate-limiting step and the pseudo-second-order model based on chemical adsorption as the rate-limiting step. The equations of the above two kinetics models can be respectively shown in Equations (2) and (3).

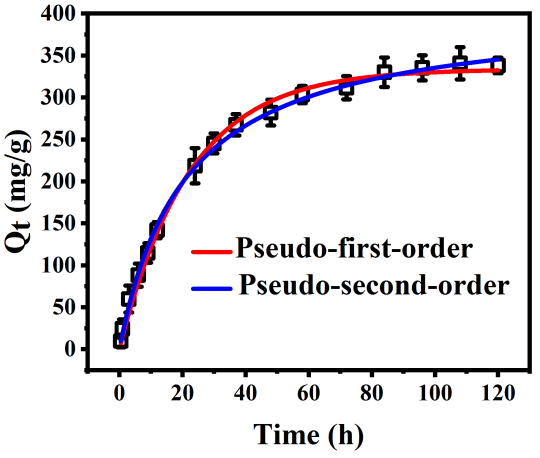

Figure 5. Adsorption performance of AO-PENFM adsorbents in12 ppm uranium spiked solution according to the pseudo-first-order model and pseudo-second-order model.

Pseudo-first-order model:

$$\ln(Q_e - Q_t) = \ln Q_e - k_1 t \quad (2)$$

Pseudo-second-order model:

$$\frac{t}{Q_t} = \frac{1}{k_2 Q_e} + \frac{t}{Q_e} \quad (3)$$

where Q_e(mg/g) is the uranium adsorption capacity at equilibrium time and Q_t (mg/g) is the uranium adsorption capacity at contact time; t(h) is contact time; k_1(1/h) is the rate constant of the pseudo-first-order model and k_2(g/(mg · h)) is the rate constant of the pseudo-second-order model.

As shown in Figure 5 and Table 1, the kinetics parameters of the above two models for simulating the uranium adsorption behavior are listed. The pseudo-first-order model with a correlation coefficient (R^2) of 0.9971 is lower than the pseudo-second-order model with R^2 of 0.9982, which indicates that the pseudo-second-order model better described the adsorption process. In other words, the rate-limiting step is the chemical adsorption of uranium adsorption.

The adsorption kinetics can also be described by the intraparticle diffusion model and the liquid membrane diffusion model. The equations can be shown respectively in Equations (4) and (5):

Intraparticle diffusion model

$$Q_t = k_i t^{1/2} + C \quad (4)$$

Liquid membrane diffusion model

$$\ln\left(1 - \frac{Q_t}{Q_e}\right) = -k_l t \quad (5)$$

where k_i(mg/(g · $h^{1/2}$)) is the rate constant of the intraparticle diffusion model, k_l (1/h) is the rate constant of the liquid membrane diffusion model and C (mg/g) is the constant.

As shown in Figure 6(a) and Table 2, the adsorption curve consists of three distinct slope sections according to the intraparticle diffusion model. The first phase lasts from 0 to 37 h, and this phase includes the external surface mass transfer, instantaneous adsorption process and the migration of uranium from the aqueous solution to AO-PENFM. Then the second phase lasts from 37 to 84 h. This phase is mainly an intraparticle diffusion process and the adsorption kinetic process between uranium and AO groups on AO-PENFM is included. And the third phase is an adsorption equilibrium stage[31]. These results show that the intraparticle diffusion model also fits the adsorption process well, and the intraparticle diffusion is also the rate-limiting step.

As shown in Figure 6(b), from 0 to 37 h, the fitting results indicate that the adsorption process is controlled by the liquid membrane diffusion model, which is characterized by the external surface mass transfer, instantaneous adsorption stage and the migration of uranium from the aqueous solution to AO-PENFM. However, in the later stage, the adsorption process is more suitable to be explained by the intraparticle diffusion model.

Meanwhile, the adsorption experiments of PENFM, PENFM-g-PHEA, PENFM-g-PHEA-(PAN-co-PAA) and AO-PENFM were performed under the same

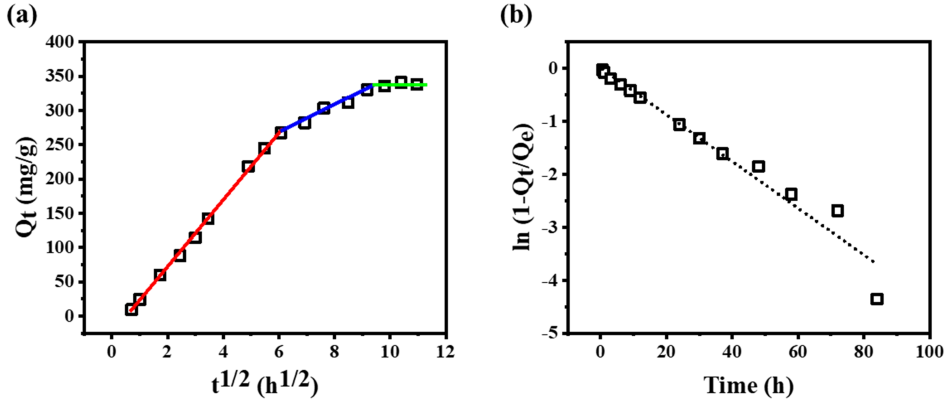

Figure 6. Adsorption performance of AO-PENFM adsorbents in 12 ppm uranium spiked solution according to (a) intraparticle diffusion model and (b) liquid membrane diffusion model.

Table 1. Kinetics fitting results for uranium adsorption on AO-PENFM according to the pseudo-first-order model and pseudo-second-order model.

Adsorbent	Pseudo-first-order model			Pseudo-second-order model		
	Q_e(mg/g)	k_1(1/h)	R^2	Q_e(mg/g)	k_2(L/g)	R^2
AO-PENFM	333.76	0.04504	0.9971	405.16	0.04802	0.9982

Table 2. Kinetics fitting results for uranium adsorption on AO-PENFM according to intraparticle diffusion model and liquid membrane diffusion model.

Adsorbent	Intraparticle diffusion model			liquid membranediffusionmodel		
	C(mg/g)	k_i(mg/(g·h$^{1/2}$))	R^2	Q_e(mg/g)	k_l(1/h)	R^2
AO-PENFM	−124.8380	148.8703	0.9815	333.76	0.04504	0.9605

conditions. The results showed that the AO-PENFM has the best adsorption efficiency and a high adsorption capacity for uranium as shown in Figure 7 (left axis). The specific surface areas of PENFM, PENFM-g-PHEA, PENFM-g-PHEA-(PAN-co-PAA) and AO-PENFM are 20.3830, 10.7606, 9.2994 and 2.0325 m^2/g, respectively. The decrease of specific surface areas is mainly caused by the densification of the material surface, which can be easily proved by SEM. And the normalized adsorption performance is calculated as shown in Figure 7 (right axis). Although the specific surface area of the AO-PENFM is reduced, the normalized adsorption performance is greatly improved. The AO-PENFM is a highly efficient uranium adsorbent.

3.2.2 Adsorption isotherm study

For the adsorption isotherm study, experiments were performed in 1 L aqueous solution containing a series of different uranium concentrations at 25 ℃ and 100 r/min, and the results were simulated by using the Freundlich and Langmuir isotherm model. The equations of the above two models can be respectively shown in Equation (6) and (7).

Langmuir isotherm model:

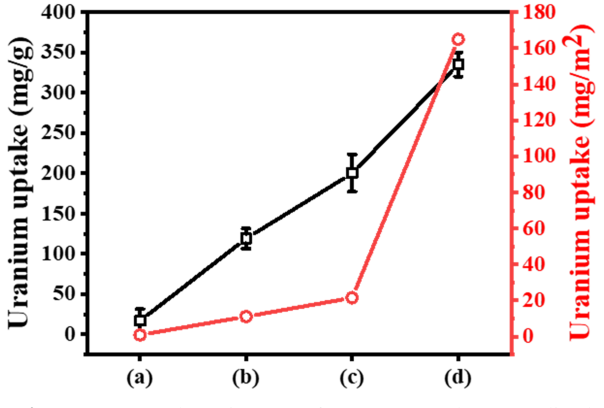

Figure 7. Adsorption performance and normalized adsorption performance of (a) PENFM, (b) PENFM-g-PHEA, (c) PENFM-g-PHEA-(PAA-co-PAN) and (d) AO-PENFM adsorbents in 12 ppm uranium spiked solution.

$$\frac{C_e}{Q_e} = \frac{C_e}{q_m} + \frac{1}{Q_m K_L} \tag{6}$$

Freundlich isotherm model:

$$Q_e = K_F C_e^{\frac{1}{n}} \tag{7}$$

where K_L (L/mg) is constant related to adsorption energy and Q_m(mg/g) is saturate adsorption capacity; K_F((mg/g)·(L/mg)$^{1/n}$) is constant related to the adsorption capacity and n is an empirical parameter related to adsorption intensity; C_e (mg/L) is the uranium concentration at equilibrium and Q_e(mg/g) is the uranium adsorption capacity of the adsorbent at equilibrium.

As shown in Figure 8(a), the adsorption isotherm curve shows that with the increase of the initial uranium concentration, uranium adsorbed on AO-PENFM begins to increase and finally reaches a plateau stage, indicating that the adsorption capacity of AO-PENFM reaches the maximum. The fitting results in Table 3 show that the Langmuir isotherm model well described the equilibrium adsorption process with R^2 of 0.9743 and further indicate that the adsorption behavior is the monolayer adsorption with a finite number of homogeneous sites on a homogeneous surface[31].

Furthermore, the values of R_L(Langmuir separation coefficient) and θ (Langmuir surface coverage rate) are used to estimate the suitability of the AO-PENFM adsorbent and understand the adsorption behavior. The equations of the R_L and θ can be shown in Equation (8) and (9):

Langmuir separation coefficient

$$R_L = \frac{1}{1 + K_L C_0} \tag{8}$$

Langmuir surface coverage rate

$$\theta = \frac{K_L C_0}{1 + K_L C_0} \tag{9}$$

where $R_L > 1$, $R_L = 1$, $0 < R_L < 1$ and $R_L = 0$ represent unsuitable, linear, suitable and irreversible, respectively. Another important factor of the uranium adsorption behavior onto AO-PENFM, is the θ, which is related to the initial uranium concentration[44].

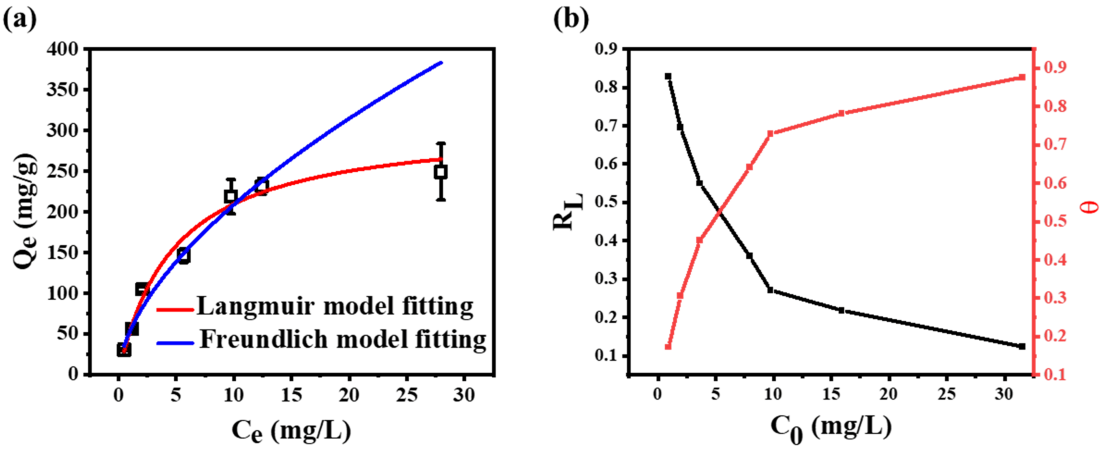

Figure 8. (a) Adsorption isotherms of AO-PENFM adsorbents fitted with Langmuir isotherm model and Freundlich equation, and (b) two parameters of the Langmuir isotherm model (R_L and θ).

Table 3. Isotherm fitting results for uranium adsorption on AO-PENFM.

Adsorbent	Langmuir parameters			Freandlich parameters		
	Q_m(mg/g)	K_L(L/mg)	R^2	n	K_F(L/g)	R^2
AO-PENFM	309.88	0.2091	0.9743	1.6907	53.5018	0.9276

As shown in Figure 8(b) that all the R_L values (0.1253−0.8305) are between 0 and 1, indicating that the AO-PENFM adsorbent has good applicability for adsorbing uranium from the solution. Meanwhile, it can be clearly seen that uranium are rapidly adsorbed by AO-PENFM adsorbent at the early stage and then tends to be a plateau. In the initial stage, due to the existence of sufficient adsorption sites, the adsorbent has a rapid adsorption rate to uranium. Then, the adsorption sites are heavily occupied, which leads to the decrease of adsorption rate, and finally to the plateau stage. This indicates that the Langmuir isotherm model well described the equilibrium adsorption process[44].

3.2.3 Reusability of the AO-PENFM adsorbent

The reusability of AO-PENFM adsorbents is performed for six adsorption-desorption cycles as shown in Figure 9. After six cycles in the solution containing 12 ppm uranium, the adsorption performance of the AO-PENFM adsorbent to uranium decreased by 8.67%, 15.01%, 13.37%, 17.53% and 21.00%, respectively, but still maintained a relatively high adsorption. The results show that the AO-PENFM adsorbent has good reusability and is of great significance for the actual adsorption of uranium.

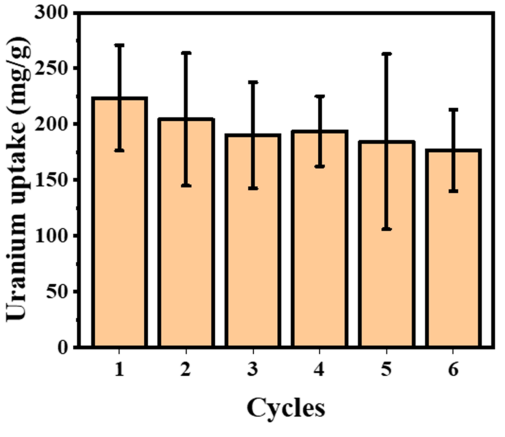

Figure 9. Uranium adsorption performance in 12 ppm uranium spiked solution for 24 h during six adsorption-desorption cycles.

4 Conclusions

In this study, a novel amidoxime-modified PENFM adsorbent is synthesized via RIGP and CIGP. The AO-PENFM has a unique nanostructure adsorption layer with high specific surface area. Therefore, a mass of adsorption sites were formed on the membrane surface. The uranium adsorption capacity in a uranium solution of 12 ppm after 120 h adsorption is 338.14 mg/g. Moreover, the adsorption kinetics conforms to the intraparticle diffusion model and pseudo-second-order model, and the adsorption isotherm data conform to the Langmuir isotherm model. The AO-PENFM adsorbent has an excellent uranium adsorption performance, which shows great application potential in supporting the nuclear power generation in the future.

Acknowledgments

This work was supported by the National Natural

Science Foundation of China (51890872, 51633009).

Conflict of interest

The authors declare no conflict of interest.

Author information

YU Rui is currently a PhD student in National Synchrotron Radiation Laboratory under the supervision of Prof. LI Liangbin at University of Science and Technology of China. His research mainly focuses on surface modification of polyolefin materials and uranium adsorption.

CHEN Xin (corresponding author) received her PhD from University of Science and Technology of China. She is currently a postdoctoral fellow at University of Science and Technology of China. Her research interests are functional modification and application of polymer films.

LI Liangbin (corresponding author) received his PhD from Sichuan University. He is currently a professor at University of Science and Technology of China. His research interests include the development of synchrotron radiation time-space energy resolution techniques and in-situ research methods, as well as in situ studies of processing-structure-property relationships of polymer materials.

References

[1] Chu S, Majumdar A. Opportunities and challenges for a sustainable energy future. Nature, 2012, 488(7411): 294-303.

[2] Hoffert M I, Caldeira K, Benford G, et al. Advanced technology paths to global climate stability: energy for a greenhouse planet. Science, 2002, 298(5595): 981-987.

[3] Abney C W, Mayes R T, Saito T, et al. Materials for the recovery of uranium from seawater. Chemical Reviews, 2017, 117(23): 13935-14013.

[4] Hu J, Ma H, Xing Z, et al. Preparation of amidoximated ultrahigh molecular weight polyethylene fiber by radiation grafting and uranium adsorption test. Industrial & Engineering Chemistry Research, 2015, 55(15): 4118-4124.

[5] Sugasaka K, Katoh S, Takai N, et al. Recovery of uranium from seawater. Separation Science and Technology, 2006, 16(9): 971-985.

[6] Kabay N, Demircioglu M, Yayli S, et al. Recovery of uranium from phosphoric acid solutions using chelating ion-exchange resins. Industrial & Engineering Chemistry Research, 1998, 37(5): 1983-1990.

[7] Tabushi I, Kobuke Y, Nishiya T. Extraction of uranium from seawater by polymer-bound macrocyclic hexaketone. Nature, 1979, 280(5724): 665-666.

[8] Liu C, Hsu P C, Xie J, et al. A half-wave rectified alternating current electrochemical method for uranium extraction from seawater. Nature Energy, 2017, 2(4): 17007.

[9] Luo W, Kelly S D, Kemner K M, et al. Sequestering uranium and technetium through co-precipitation with aluminum in a contaminated acidic environment. Environmental Science & Technology, 2009, 43(19): 7516-7522.

[10] Das S, Brown S, Mayes R T, et al. Novel poly(imide dioxime) sorbents: Development and testing for enhanced extraction of uranium from natural seawater. Chemical Engineering Journal, 2016, 298: 125-135.

[11] Das S, Oyola Y, Mayes R T, et al. Extracting uranium from seawater: Promising AF series adsorbents. Industrial & Engineering Chemistry Research, 2015, 55(15): 4110-4117.

[12] Li Y, Wang L, Li B, et al. Pore-free matrix with cooperative chelating of hyperbranched ligands for high-performance separation of uranium. ACS Applied Materials Interfaces, 2016, 8(42): 28853-28861.

[13] Liu X, Liu H, Ma H, et al. Adsorption of the uranyl ions on an amidoxime-based polyethylene nonwoven fabric prepared by preirradiation-induced emulsion graft polymerization. Industrial & Engineering Chemistry Research, 2012, 51(46): 15089-15095.

[14] Ma C, Gao J, Wang D, et al. Sunlight polymerization of poly(amidoxime) hydrogel membrane for enhanced uranium extraction from seawater. Advanced Science, 2019, 6(13): 1900085.

[15] Oyola Y, Dai S. High surface-area amidoxime-based polymer fibers co-grafted with various acid monomers yielding increased adsorption capacity for the extraction of uranium from seawater. Dalton Transactions, 2016, 45(21): 8824-8834.

[16] Pan H B, Wai C M, Kuo L J, et al. A highly efficient uranium grabber derived from acrylic fiber for extracting uranium from seawater. Dalton Transactions, 2020, 49(9): 2803-2810.

[17] Qian J, Zhang S, Zhou Y, et al. Synthesis of surface ion-imprinted magnetic microspheres by locating polymerization for rapid and selective separation of uranium(VI). RSC Advances, 2015, 5(6): 4153-4161.

[18] Saito T, Brown S, Chatterjee S, et al. Uranium recovery from seawater: development of fiber adsorbents prepared via atom-transfer radical polymerization. Journal of Materials Chemistry A, 2014, 2(35): 14674-14681.

[19] Sun Q, Aguila B, Perman J, et al. Bio-inspired nano-traps for uranium extraction from seawater and recovery from nuclear waste. Nature Communications, 2018, 9(1): 1644.

[20] Wang D, Song J, Wen J, et al. Significantly enhanced uranium extraction from seawater with mass produced fully amidoximated nanofiber adsorbent. Advanced Energy Materials, 2018, 8(33): 1802607.

[21] Xiong J, Hu S, Liu Y, et al. Polypropylene modified with amidoxime/carboxyl groups in separating uranium(VI) from thorium(IV) in aqueous solutions. ACS Sustainable Chemical Energy, 2017, 5(2): 1924-1930.

[22] Xu M, Han X, Hua D. Polyoxime-functionalized magnetic nanoparticles for uranium adsorption with high selectivity over vanadium. Journal of Materials Chemistry A, 2017, 5(24): 12278-12284.

[23] Xu X, Ding X-J, Ao J X, et al. Preparation of amidoxime-based PE/PP fibers for extraction of uranium from aqueous solution. Nuclear Science and Techniques, 2019, 30(2): 38-50.

[24] Xu X, Xu L, Ao J X, et al. Ultrahigh and economical uranium extraction from seawater via interconnected open-pore architecture poly(amidoxime) fiber. Journal of Materials Chemistry A, 2020, 8(42): 22032-22044.

[25] Yang S, Qian J, Kuang L, et al. Ion-imprinted mesoporous silica for selective removal of uranium from highly acidic and radioactive effluent. ACS Applied Materials Interfaces, 2017, 9(34): 29337-29344.

[26] Yue Y, Mayes R T, Kim J, et al. Seawater uranium sorbents: Preparation from a mesoporous copolymer initiator by atom-transfer radical polymerization. Angewandte

Chemie, 2013, 52(50): 13458-13462.
[27] Zhao S, Yuan Y, Yu Q, et al. A dual-surface amidoximated halloysite nanotube for high-efficiency economical uranium extraction from seawater. Angewandte Chemie, 2019, 58(42): 14979-14985.
[28] Zhou L, Bosscher M, Zhang C, et al. A protein engineered to bind uranyl selectively and with femtomolar affinity. Nature Chemistry, 2014, 6(3): 236-241.
[29] Chatterjee S, Bryantsev V S, Brown S, et al. Synthesis of naphthalimidedioxime ligand-containing fibers for uranium adsorption from seawater. Industrial & Engineering Chemistry Research, 2015, 55(15): 4161-4169.
[30] Das S, Brown S, Mayes R T, et al. Novel poly(imide dioxime) sorbents: Development and testing for enhanced extraction of uranium from natural seawater. Chemical Engineering Journal, 2016, 298: 125-135.
[31] Lu X, Zhang D, Tesfay Reda A, et al. Synthesis of amidoxime-grafted activated carbon fibers for efficient recovery of uranium(VI) from aqueous solution. Industrial & Engineering Chemistry Research, 2017, 56(41): 11936-11947.
[32] Xu X, Zhang H, Ao J, et al. 3D hierarchical porous amidoxime fibers speed up uranium extraction from seawater. Energy Environment Science, 2019, 12(6): 1979-1988.
[33] Das S, Tsouris C, Zhang C, et al. Enhancing uranium uptake by amidoxime adsorbent in seawater: An investigation for optimum alkaline conditioning parameters. Industrial & Engineering Chemistry Research, 2015, 55(15): 4294-4302.
[34] Chen L, Bai Z, Zhu L, et al. Ultrafast and efficient extraction of uranium from seawater using an amidoxime appended metal-organic framework. ACS Applied Material Interfaces, 2017, 9(38): 32446-32451.
[35] Jiao C, Zhang Z, Tao J, et al. Synthesis of a poly(amidoxime-hydroxamic acid) cellulose derivative and its application in heavy metal ion removal. RSC Advances, 2017, 7(44): 27787-27795.
[36] Yan B, Ma C, Gao J, et al. An ion-crosslinked supramolecular hydrogel for ultrahigh and fast uranium recovery from seawater. Advanced Materials, 2020, 32(10): e1906615.
[37] Brown S, Chatterjee S, Li M, et al. Uranium adsorbent fibers prepared by atom-transfer radical polymerization from chlorinated polypropylene and polyethylene trunk fibers. Industrial & Engineering Chemistry Research, 2015, 55(15): 4130-4138.
[38] Brown S, Yue Y, Kuo L J, et al. Uranium adsorbent fibers prepared by atom-transfer radical polymerization (ATRP) from poly(vinyl chloride)-co-chlorinated poly(vinyl chloride) (PVC-co-CPVC) fiber. Industrial & Engineering Chemistry Research, 2016, 55(15): 4139-4148.
[39] Das S, Oyola Y, Mayes R T, et al. Extracting uranium from seawater: Promising AI series adsorbents. Industrial & Engineering Chemistry Research, 2015, 55(15): 4103-4109.
[40] Chen X, Wan C, Yu R, et al. Fabrication of amidoximated polyacrylonitrile nanofibrous membrane by simultaneously biaxial stretching for uranium extraction from seawater. Desalination, 2020, 486: 114447.
[41] Ma F, Dong B, Gui Y, et al. Adsorption of low-concentration uranyl ion by amidoxime polyacrylonitrile fibers. Industrial & Engineering Chemistry Research, 2018, 57(51): 17384-17393.
[42] Wan C, Chen X, Lyu F, et al.. Biaxial stretch-induced structural evolution of polyethylene gel films: Crystal melting recrystallization and tilting. Polymer, 2019, 164: 59-66.
[43] Wan C, Cao T, Chen X, et al. Fabrication of polyethylene nanofibrous membranes by biaxial stretching. Materials Today Communications, 2018, 17: 24-30.
[44] Bai Z, Liu Q, Zhang H, et al. A novel 3D reticular anti-fouling bio-adsorbent for uranium extraction from seawater: Polyethylenimine and guanidyl functionalized hemp fibers. Chemical Engineering Journal, 2020, 382: 122555-122564.

改性聚乙烯纳米纤维膜用于铀吸附的应用研究

余瑞[1], 万彩霞[1], 陈鑫[1,2*], 李良彬[1*]

1. 中国科学技术大学国家同步辐射实验室, 安徽省先进功能高分子薄膜工程实验室, 中国科学院软物质化学重点实验室, 安徽合肥 230026;
2. 西南科技大学核废料处理与环境安全国家协同创新中心, 四川绵阳 621010

* 通讯作者. E-mail: cx1003@ustc.edu.cn; lbli@ustc.edu.cn

摘要: 以聚乙烯纳米纤维膜为基膜,通过预辐照触发接枝丙烯酸羟乙酯,随后通过硝酸铈铵引发在聚丙烯酸羟乙酯链上接枝丙烯腈和丙烯酸,最后进行胺肟化反应, 合成一种新的偕胺肟基纳米纤维膜吸附剂,并将其命名为 AO-PENFM. 通过两步接枝的方法可以在聚乙烯膜表面构筑大比表面积的纳米结构吸附层. AO-PENFM 的吸附行为使用 12 ppm 的铀加标溶液进行测试. 在 100 r/min 的 25 ℃恒温水浴摇床中吸附 120 h,AO-PENFM 对铀的吸附能力为 338. 14 mg/g. AO-PENFM 吸附剂对铀的吸附动力学很好地符合离子扩散模型和拟二级动力学模型,同时吸附等温线数据很好地满足 Langmuir 模型.

关键词: 聚乙烯纳米纤维膜;预辐照触发接枝聚合;硝酸铈铵引发接枝聚合;铀吸附